Optics Letters

Widely bandwidth-tunable silicon filter with an unlimited free-spectral range

Jonathan St-Yves, Hadi Bahrami, Philippe Jean, Sophie LaRochelle, and Wei Shi*

*Centre d'optique, photonique et laser (COPL) and Département de génie électrique et génie informatique, Université Laval,
2375 rue de la Terrasse, Québec G1 V 0A6, Canada*
Corresponding author: wei.shi@gel.ulaval.ca

Next-generation high-capacity optical networks require flexible allocation of spectrum resources, for which low-cost optical filters with an ultra-wide bandwidth tunability beyond 100 GHz are desired. We demonstrate an integrated band-pass filter with the bandwidth continuously tuned across 670 GHz (117–788 GHz) which, to the best of our knowledge, is the widest tuning span ever demonstrated on a silicon chip. The filter also features simultaneous wavelength tuning and an unlimited free spectral range. We measured an out-of-band contrast of up to 55 dB, low in-band ripples of less than 0.3 dB, and in-band group delay variation of less than 8 ps. This result was achieved using cascaded Bragg-grating-assisted contra-directional couplers and micro-heaters on the 220 nm silicon-on-insulator platform with a very compact footprint of less than 7000 μm^2. Another design with the bandwidth continuously tunable from 50 GHz to 1 THz is also presented. © 2015 Optical Society of America

Next-generation optical transmission systems applying flexible networking and the super-channel technique will require highly dynamic channel allocation to drastically increase the spectral efficiency and transmission capacity [1,2]. Tunable optical filters, reconfigurable in both center wavelength and bandwidth with scalability toward terahertz [2], are essential for these applications. Such large bandwidth tunability is currently only available in bulky bench-top systems using diffractive grating spectrometers or liquid crystals. Integrated solutions are desired for lower cost and power consumption. In particular, silicon photonics based on the sub-micron silicon-on-insulator platform allows for CMOS compatible mass fabrication, enabling low-cost, high-yield, and high-density chip-scale integration. Existing solutions for tunable filters on silicon include devices based on microring resonators [3,4] and Mach–Zehnder interferometers (MZIs). These devices have relatively small tunable bandwidths (less than 200 GHz) and small free spectral ranges

(FSR), typically less than 10 nm, unable to cover the entire C-band, which are not suitable for high-capacity transmission applications.

Contra-directional couplers (contra-DCs) are grating assisted add-drop filters [5]. Analogous to waveguide Bragg gratings, the wavelength selectivity in contra-DCs is based on periodic dielectric perturbations. However, instead of back reflections in the same waveguide, the selected wavelength in a contra-DC is dropped to another waveguide through contra-directional coupling. This allows add-drop operation without the need of a circulator. Contra-DCs have merits of compactness, flat-top response, flexible filter design (e.g., through apodization), and near-infinite FSR (in the case of first-order gratings). In particular, they allow for very high bandwidths (greater than 10 nm) and, thus, can support very high baud rate super-channel signals [1]. In this Letter, we demonstrate a broadband filter with a large tunability in both wavelength and channel bandwidth, using thermally controlled cascaded contra-DCs on a silicon chip. The filter has flat-top responses, low insertion loss, low in-band ripples, and high contrast between the pass-band and the stop-band.

The schematic of the proposed device is shown in Fig. 1. It consists of a pair of cascaded contra-DCs, each operating as a drop filter. The drop port of the first contra-DC is connected to the input port of the second contra-DC. Therefore, the finally dropped signal ("drop port of the system") is determined
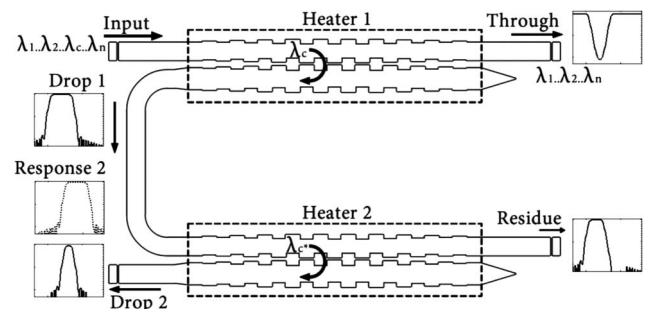

Fig. 1. Schematic of the device. The dropped wavelength of the first contra-DC is re-filtered in an identical component. Both contra-DCs are temperature controlled with metal heaters. Plots show examples of spectra at each port on a logarithmic scale.

by the product of the drop-port transfer functions of the two contra-DCs.

At first, the two filters are identical and drop a large, well-defined window. By changing the temperature of a single filter, the bandwidth of the finally dropped signal can be adjusted by detuning the center wavelengths of the two contra-DCs.

A broadband filter design for a coarse WDM on 220 nm SOI [6] is adopted for individual contra-DCs. In each contra-DC, the widths of the waveguides are 560 and 440 nm. This high asymmetry ensures a negligible forward cross-coupling. The gratings are formed by sidewall corrugations in strip waveguides with a pitch of 312 nm. Each contra-DC has 1000 grating elements for a length of 312 μm. The spacing between the waveguides varies between 65 and 135 nm to produce a Gaussian-profiled coupling apodization, as shown in Fig. 2, for efficient sidelobe suppression, for which details can be found in [6].

The spectral responses of each contra-DC are calculated using the coupled mode theory and the transfer matrix method, following the same procedure as in [5], with three additions: apodization, temperature dependence, and noise simulation. While an unapodized (uniform) grating can be simulated with only two transfer matrices, an apodized design needs an independent matrix for each grating element along the propagation to match the change of coupling, and the transfer matrix of the entire contra-DC is given by the product of all the grating elements along the propagation axis. Our simulations use 100 segments to approximate the continuously varied coupling.

On top of each contra-DC sits a metal strip acting as a micro-heater for thermal tuning. The refractive index of silicon has a temperature dependence of $dn_{Si}/dT = 1.87 \times 10^{-4}$ K^{-1} at room temperature for wavelengths around 1550 nm [7]. Without electrical input, the optical responses of the two filters are, in principle, identical (except for fabrication errors), resulting in a sharp transition from the pass-band to the stop-band. Applying independent electrical currents on the heaters, we can shift the spectra of the contra-DCs simultaneously or differentially for wavelength or bandwidth tuning. Ideally, each contra-DC should be uniformly heated so that the apodization profile would not be disturbed as the temperature varies. In simulation, the temperature dependence is accounted for by $dn_{eff} = dn_{Si}/dT \times dn_{eff}/dn_{Si} \times dT$, where dn_{eff}/dn_{Si} is evaluated using an eigenmode solver.

While only coupling apodization has been discussed so far, it is common in Bragg grating profiles to also adjust the local Bragg wavelength. This can be done with a phase shift changing the local effective index or period. This design only uses coupling apodization, in principle, but phase noise also appears during fabrication due to nonuniformity and sidewall roughness.

There are two main types of waveguide noise considered in our simulation. High-frequency phase noise (typically around 10 μm of the spatial period [8]) is caused by sidewall roughness and decreases the sidelobe suppression. Low-frequency phase noise, with a correlation length larger than the device (300 μm), is caused by the wafer thickness nonuniformity and etching variance, resulting in a linear chirp that increases the bandwidth. High-frequency phase noise is considered in our simulation by adding random noise $\Delta\hat{\beta}$ to the propagation constants. The frequency distribution of the noise thus matches the quantization steps of the matrices but, since the response noise is dependent on both the amplitude and frequency of the sidewall roughness [9], we can fit the simulation to the experiment by choosing the right noise amplitude. Similarly, we can also add a variation to $\Delta\hat{\beta}$ which is dependent on the longitudinal position.

Fig. 3. Spectral response of the cascaded filters without heating: 1 dB BW is 733 GHz, 3 dB BW is 788 GHz, 10 dB BW is 868 GHz, and 20 dB BW is 990 GHz. The inset shows the filter shape near the center wavelength.
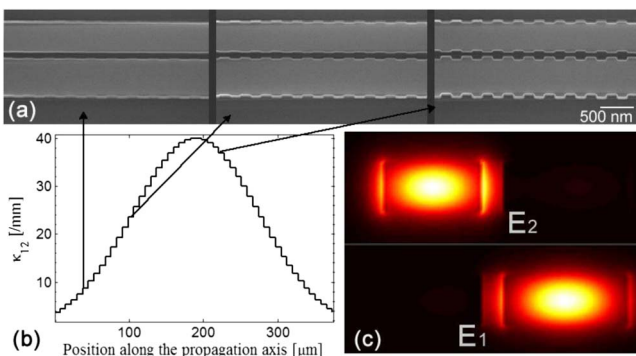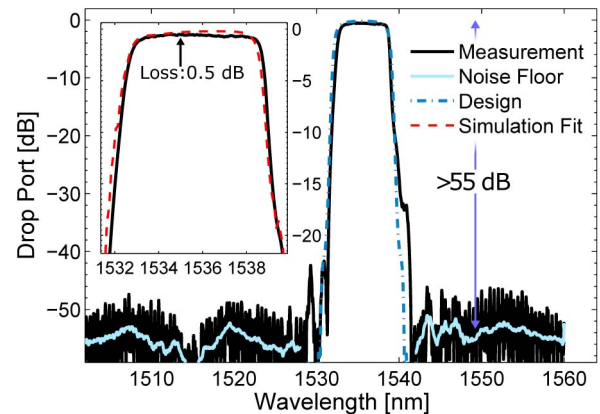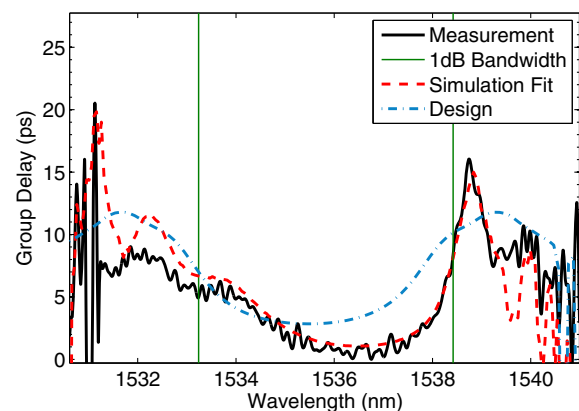

Fig. 2. (a) SEM photography of a part of the grating. The contra-DC consists of two close waveguides of different width with periodic sidewall corrugations. (b) Apodization profile of the grating. A larger coupling requires larger corrugations. (c) Intensity distributions of electrical fields of the first and second transverse modes.

Fig. 4. Group delay response of the tunable filter at the drop port. The delay stays within 8 ps between any two points in the band. The out of band results are noisy due to the weak signal.
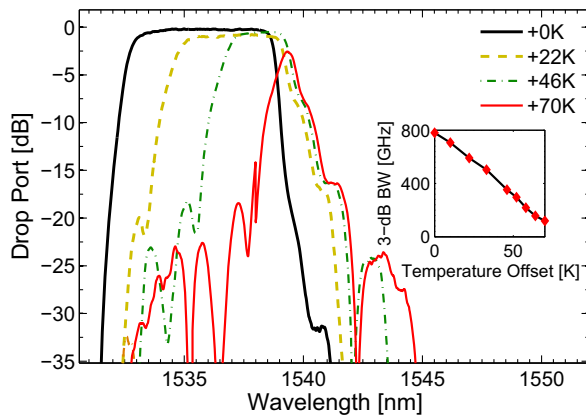
Fig. 5. Spectral response of the device for different temperatures applied to only one contra-DC: 1 dB BW tuned down to 65 GHz, 3 dB BW tuned down to 117 GHz. The temperatures are obtained from simulation fit. The inset shows the temperature dependence.
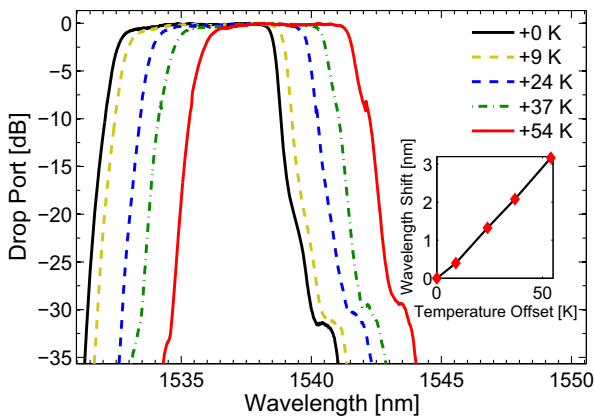

Fig. 6. Spectral response with the heat applied to both contra-DCs: the central wavelength is tuned from 1535 to 1539 nm continuously; the temperatures are calculated by comparison to simulation. The inset shows the temperature dependence.

The device was fabricated using a CMOS-compatible technology with electron–beam lithography. Scanning electron microscope (SEM) images at various positions along the apodization profile are shown in Fig. 2(a). Large coupling coefficients and precise apodization profiles can also be achieved using UV lithography, where the smoothing effect needs to be carefully calibrated. The corrugations do not need to be squared shaped, but must have a sufficient amplitude. Fiber grating couplers [10] are used as optical inputs and outputs in the measurement. Figure 3 shows the measured drop-port response of the cascaded contra-DC

filters. The measurements were normalized using the response of a pair of directly connected fiber grating couplers on the same chip.

The device exhibits a high sidelobe suppression ratio (SLSR) of over 40 dB and a high contrast of about 55 dB between the pass-band and the stop-band. The insertion loss is very low, less than 0.5 dB (i.e., 0.25 dB per contra-DC), with small ripples of less than 0.3 dB within the 1 dB passband over 5.8 nm (733 GHz). A loss of 8 dB/cm has been used in our simulation that shows good agreement with the experiment. However, we can expect a lower loss using optical lithography, which produces smoother waveguide sidewalls and, thus, lower optical scatterings [11]. The edge roll-off rate is 19 dB/nm on the left side and 24 dB/nm on the right side.

Another important parameter to monitor is the group delay, as an uneven delay within the pass band may cause signal distortion. The simulation and measurements seen in Fig. 4 show a group delay difference of less than 8 ps within the 1 dB bandwidth. Compared to the original design without considering the phase noise due to fabrication errors, the measured group delay shows a slight distortion. Good agreement is obtained by taking into consideration the linear chirp caused by the silicon wafer thickness variation. Further work could optimize the grating structure more using the inverse layer peeling algorithm [12] since the mathematics of the contra-DC is similar to that of the Bragg gratings.

By changing the temperature of a single contra-DC, we shift its phase-match condition, resulting in a smaller band overlap between the two contra-DCs and, thus, a narrower passband in the drop port, as shown in Fig. 5. A continuous tuning of the 3 dB bandwidth from 788 GHz down to 117 GHz (i.e., over 670 GHz or 5.4 nm) is experimentally observed as the on-chip temperature increases by 70°. Due to the wavelength detuning, the stop-band edges are now determined by the single filters. As a result, the SLSR degrades to −15 dB at the smallest bandwidth.

The power efficiency of the bandwidth tuning is about 24 mW/nm. This relatively low efficiency is partially due to the use of a bulky heater made of 300 nm thick, 2 µm wide Al strips. We also observe a slight redshift of the center wavelength at a higher temperature, indicating thermal coupling between the two contra-DCs that are about 10 µm away from each other. The tuning efficiency can be significantly improved by optimizing the heater design, e.g., using smaller heater features and thermal isolation [13].

By applying the same temperature variation to both contra-DCs, the center wavelength can be tuned without affecting the filter shape. As shown in Fig. 6, when the center wavelength is continually changed over 4 nm by varying the on-chip temperature, the filter shape is maintained with sharp edges. The power efficiency of the wavelength tuning is about 44 mW/nm, which is about twice the power consumption of the bandwidth tuning since two contra-DCs are heated simultaneously.

Table 1. Recent Results with Multi-Element On-Chip Silicon Filters

| Publication	Filter Type	BWmax/FSR	Tunable BW	On-Chip Loss/Ripples	Contrast
Ding *et al.* [14]	MRs + MZI	55 GHz/1 THz	28–55 GHz	3.6 dB/1 dB	30 dB
Orlandi *et al.* [15]	MRs + MZI	173 GHz/200 GHz	23–173 GHz	0.46–1.06 dB/0.5 dB	15–34 dB
Ong *et al.* [4]	Cascaded MRs	125 GHz/0.9 THz	11.6–125 GHz	0.25 dB/3 dB	50–100 dB
This Experiment	Cascaded contra-DC	778 GHz/Unlimited	67–778 GHz	0.5 dB/0.3 dB	15–55 dB
4-Stage Design	Cascaded contra-DC	1 THz/Unlimited	49–1007 GHz	<1 dB/0.3 dB	>49 dB
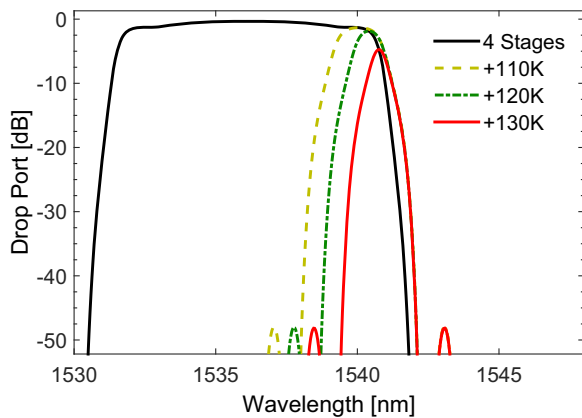
Fig. 7. Simulation of the spectral response with the heat applied to two out of four cascaded contra-DCs: the 1 dB bandwidth can be continuously tuned from 1007 to 49 GHz. The sidelobes stay under –49 dB, even for small bandwidths due to the double filtering. This simulation does not consider fabrication phase noise.

Table 1 shows a comparison of recent publications of tunable optical filters on the SOI platform. Our device shows the highest tunable bandwidth and is the only one that allows for a bandwidth beyond 200 GHz. It is noteworthy that the other devices all have a small FSR less than the span of the C-band (35 nm), while our device does not suffer from a limited FSR. This indicates a unique capacity for dynamic allocation of spectrum resources. In addition, our device is, to the best of our knowledge, among the best in terms of loss ripples and contrast.

For improved performance and flexibility, more stages can be cascaded. Figure 7 shows our simulation results for a four-stage cascade contra-DC filter, consisting of two pairs of identical contra-DCs with a stronger coupling than the one experimentally demonstrated (53.5 mm^{-1} versus 38 mm^{-1}). Each pair is controlled by the same temperature, performing as a single tuning element.

In summary, we have demonstrated a bandwidth tunable filter with a low insertion loss of less than 0.5 dB, low ripples of less than 0.3 dB, a large maximal bandwidth of greater than 750 GHz, and high contrast of 55 dB. A large bandwidth tuning range over 670 GHz has been achieved which, to the best of our knowledge, is the widest ever demonstrated on a silicon chip. This ultra-wide bandwidth tunability makes the device very attractive for next-generation ultrahigh baud rate applications (e.g., high-capacity super-channel transmissions) and flexible optical networking.

REFERENCES

1. M. Jinno, H. Takara, B. Kozicki, Y. Tsukishima, Y. Sone, and S. Matsuoka, IEEE Commun. Mag. **47**(11), 66 (2009).
2. D. J. Geisler, N. K. Fontaine, R. P. Scott, and S. Yoo, IEEE Photon. J. **3**, 1013 (2011).
3. B. Zhang, D. Leuenberger, M.-C. M. Lee, A. Willner, and M. Wu, IEEE Photon. Technol. Lett. **19**, 1508 (2007).
4. J. R. Ong, R. Kumar, and S. Mookherjea, IEEE Photon. Technol. Lett. **25**, 1543 (2013).
5. W. Shi, X. Wang, C. Lin, H. Yun, Y. Liu, T. Baehr-Jones, M. Hochberg, N. A. Jaeger, and L. Chrostowski, Opt. Express **21**, 3633 (2013).
6. W. Shi, H. Yun, C. Lin, X. Wang, J. Flueckiger, N. Jaeger, and L. Chrostowski, *Conference on Lasers and ElectroOptics: Science and Innovations* (Optical Society of America, 2013), paper CTu3F-5.
7. B. J. Frey, D. B. Leviton, and T. J. Madison, Proc. SPIE **6273**, 62732J (2006).
8. A. D. Simard, G. Beaudin, V. Aimez, Y. Painchaud, and S. LaRochelle, Opt. Express **21**, 23145 (2013).
9. A. D. Simard, N. Ayotte, Y. Painchaud, S. Bedard, and S. LaRochelle, J. Lightwave Technol. **29**, 3693 (2011).
10. Q. Zhong, V. Veerasubramanian, Y. Wang, W. Shi, D. Patel, S. Ghosh, A. Samani, L. Chrostowski, R. Bojko, and D. V. Plant, Opt. Express **22**, 18224 (2014).
11. M. Caverley, N. A. Jaeger, and L. Chrostowski, *Photonics North* (IEEE, 2015), p. 1.
12. J. Skaar, L. Wang, and T. Erdogan, IEEE J. Quantum Electron. **37**, 165 (2001).
13. P. Dong, W. Qian, H. Liang, R. Shafiiha, D. Feng, G. Li, J. E. Cunningham, A. V. Krishnamoorthy, and M. Asghari, Opt. Express **18**, 20298 (2010).
14. Y. Ding, M. Pu, L. Liu, J. Xu, C. Peucheret, X. Zhang, D. Huang, and H. Ou, Opt. Express **19**, 6462 (2011).
15. P. Orlandi, C. Ferrari, M. J. Strain, A. Canciamilla, F. Morichetti, M. Sorel, P. Bassi, and A. Melloni, Opt. Lett. **37**, 3669 (2012).